Iranian Journal of Basic Medical Sciences
ijbms.mums.ac.ir

Eugenol attenuates paclitaxel-induced cardiotoxicity by modulating autophagy-related markers in rats

Halime Tozak Yildiz [1]*, Sadık Küçükgünay [2], Oya Korkmaz [3], Seda Koçak [4], Mustafa Numan Bucak [5]

[1] Department of Histology and Embryology, Faculty of Medicine, Kirsehir Ahi Evran University, 40100 Kirsehir, Türkiye
[2] Department of Medical Pharmacology, Faculty of Medicine, Kirsehir Ahi Evran University, 40100 Kirsehir, Türkiye
[3] Department of Histology and Embryology, Faculty of Medicine, Malatya Turgut Ozal University, 44210 Malatya, Türkiye
[4] Department of Physiology, Faculty of Medicine, Kirsehir Ahi Evran University, 40100 Kirsehir, Türkiye
[5] Department of Fertilization and Artificial Insemination, Faculty of Veterinary Medicine, Selcuk University, 42250 Konya, Türkiye

ARTICLE INFO

Article type:
Original

Article history:
Received: Jul 11, 2025
Accepted: Feb 14, 2026

Keywords:
Autophagy
Eugenol
Heart Injuries
Mechanistic target of -rapamycin complex 1
Oxidative stress
Paclitaxel
Rats

ABSTRACT

Objective(s): Paclitaxel (PTX) is a commonly used chemotherapeutic agent that causes cardiotoxicity characterized by oxidative stress, inflammation, and mitochondrial dysfunction, which disrupts autophagy and apoptosis in cardiomyocytes. This study investigated the therapeutic potential of eugenol (EUG), a natural anti-oxidant and anti-inflammatory compound, against PTX-induced cardiac damage.

Materials and Methods: Thirty-six male Wistar rats were randomly assigned to six groups: Control, EUG5, EUG25, PTX, PTX+EUG5, and PTX+EUG25. Hemodynamic parameters (systolic and diastolic blood pressure and heart rate), serum cardiac biomarkers (troponin T and brain natriuretic peptide), histopathological alterations, and immunohistochemical expression of autophagy-related proteins (mTOR, ULK1, and Atg13) were evaluated.

Results: PTX administration significantly reduced arterial blood pressure and increased serum cardiac injury biomarkers, accompanied by marked myocardial structural damage. Histopathological analysis revealed myocardial degeneration, inflammation, edema, and tissue disorganization in the PTX group. In PTX-exposed rats treated with EUG, arterial blood pressure was higher, and serum cardiac injury biomarkers were lower than in the PTX group, accompanied by reduced histopathological scores. PTX exposure was associated with decreased mTOR expression and increased ULK1 and Atg13 immunoreactivity, while EUG-treated PTX groups showed values closer to those of the control group for these autophagy-related markers.

Conclusion: EUG administration was associated with reduced biochemical and histopathological indicators of cardiac injury in PTX-exposed rats, along with changes in autophagy-related markers. These findings demonstrate that EUG treatment coincided with attenuation of PTX-induced cardiac injury at the biochemical and histopathological levels, suggesting its potential experimental value in models of chemotherapy-associated cardiotoxicity.

▶ Please cite this article as:

Tozak Yildiz H, Küçükgünay S, Korkmaz O, Koçak S, Bucak MN. Eugenol attenuates paclitaxel-induced cardiotoxicity by modulating autophagy-related markers in rats. Iran J Basic Med Sci. 2026; 29:

Introduction

Paclitaxel (PTX) is one of the most successful and widely used anticancer drugs, significantly improving survival rates in cancer patients through its unique antitumor mechanism (1). As a landmark plant-derived chemotherapeutic agent, PTX acts as a tubulin-binding drug that disrupts mitosis and induces apoptosis (2). However, the exposure of healthy cells to this chemotherapeutic agent leads to severe side effects due to organ toxicity. Among these complications, PTX-induced cardiotoxicity manifests as ischemia, hypertension, arrhythmias, and structural and functional alterations in cardiomyocyte myofibrils (3, 4).

PTX contributes to cardiotoxicity through several interrelated mechanisms, with oxidative stress playing a central role. By increasing reactive oxygen species (ROS) production, PTX disrupts redox balance, promotes mitochondrial dysfunction, and induces cardiomyocyte apoptosis, ultimately leading to impaired cardiac function (5). In addition to oxidative stress, PTX induces inflammation by upregulating pro-inflammatory cytokines such as Tumor necrosis factor-alpha (TNF-α), interleukin-1 beta (IL-1β), and interleukin-6 (IL-6), which further contribute to myocardial damage. Apoptosis is also a key process in PTX-induced cardiotoxicity, triggered through both intrinsic and extrinsic pathways (5, 6). Moreover, PTX has been shown to disrupt autophagy, a crucial mechanism for maintaining cellular homeostasis. While autophagy can be protective under stress, its dysregulation may exacerbate cardiomyocyte injury under chemotherapeutic conditions (5, 6).

***Corresponding author:** Halime Tozak yildiz. Department of Histology and Embryology, Faculty of Medicine, Kirsehir Ahi Evran University, 40100 Kirsehir, Türkiye. Tel: +90 386 280 39 00- 2546, Email: htyildiz@ahievran.edu.tr, hhalimeyildiz@hotmail.com

Eugenol (EUG), the primary active component of clove oil, has been traditionally used in Chinese medicine as a carminative, antispasmodic, antibacterial, and antiparasitic agent (7). It is particularly well known in dentistry for its local anesthetic and analgesic properties (8). Additionally, EUG has been reported to possess anti-oxidant, antimicrobial, antiseptic, anti-inflammatory, anticancer, and anti-stress properties (9, 10). By modulating multiple intracellular signaling pathways, EUG is suggested to confer potential benefits against non-communicable diseases such as cardiac, metabolic, renal, and hepatic disorders, primarily by reducing oxidative stress and inflammation (11–13). EUG exerts its protective effects primarily through its potent xidant capacity, which scavenges ROS and inhibits lipid peroxidation, thereby preventing cellular damage and inflammation. Following cellular entry, EUG particularly targets mitochondria, where it mitigates oxidative stress and inflammation while regulating mitochondrial bioenergetic processes (14).

Autophagy is a fundamental self-protective and defensive mechanism that enables the removal of harmful or toxic substances from the cell (15). It plays a crucial role in clearing ROS, misfolded proteins, and pro-inflammatory processes, thereby maintaining cellular homeostasis (16). mTOR is a key regulator of cell growth, protein synthesis, metabolic processes, and survival mechanisms. One of the classical pathways regulating autophagy is the phosphoinositide 3-kinase (PI3K)/protein kinase B (AKT)/mechanistic target of rapamycin (PI3K/AKT/mTOR) signaling pathway. PI3K/AKT signaling activates mTOR, which inhibits autophagy by reducing autophagic activity through phosphorylation (17). Unc-51-like autophagy activating kinase 1 (ULK1) plays an important role in the initiation of autophagy by forming a regulatory complex with autophagy-related protein 13 (Atg13) and focal adhesion kinase family interacting protein of 200 kDa (FIP200). Its activity is tightly regulated by AMP-activated protein kinase (AMPK) and mTOR through phosphorylation; AMPK activates ULK1 under nutrient starvation and stress, whereas mTOR inhibits ULK1 under nutrient-rich conditions, thereby suppressing autophagy initiation (18). The AMPK/mTOR/ULK1 signaling axis governs multiple cellular processes, including energy homeostasis, cell growth, and autophagy (19).

PTX induces cardiotoxicity through various cellular mechanisms, primarily involving mitochondrial dysfunction, increased reactive oxygen species (ROS) production, and apoptosis mediated by the Bax/Bcl-2 pathways (3, 6, 20). EUG, a natural xidant and anti-inflammatory agent, has been reported to protect cardiomyocytes by reducing oxidative damage and modulating cardiac electrophysiology (15, 21). However, its specific role in alleviating PTX-induced cardiotoxicity via autophagy-related signaling, particularly the mTOR-ULK1-Atg13 pathway, remains poorly understood. Therefore, this study aims to investigate the therapeutic potential of EUG in alleviating PTX-induced cardiac damage, with a focus on its modulation of autophagic mechanisms.

Materials and Methods

Ethical approval of animal use

The experiments followed the ARRIVE guidelines (Animal Research: Reporting of *In Vivo* Experiments). All experimental protocols were approved by the Local Ethic Committee of Animal Experiments of Kırşehir Ahi Evran University (approval no. 2025/06-1) in Turkiye.

Animals and experimental groups

The study was started with eight- to ten-week-old male Wistar albino rats weighing 200–250 g. The rats were kept in a 25 °C room with a 12-hr light/dark cycle, free access to water, and a standard diet from the Experimental and Clinical Research Center at Kırşehir Ahi Evran University in Kırşehir, Turkey. The adult rats were randomly divided into six groups :

Six distinct groups of rats were established for the study

1- Control group (Control): Animals received physiological saline (vehicle) via oral gavage for 10 consecutive days.

2- Eugenol 5 group (EUG5): Animals received no treatment during days 1–5 and were then administered eugenol at a dose of 5 mg/kg/day via oral gavage for 10 consecutive days, starting on day 6 (days 6–15).

3- Eugenol 25 group (EUG25): Animals received no treatment during days 1–5 and were then administered eugenol at a dose of 25 mg/kg/day via oral gavage for 10 consecutive days, starting on day 6 (days 6–15).

4- Paclitaxel group (PTX): Animals received paclitaxel (TAKSEN® Koçak Farma, 30 mg/5 ml vial) at a dose of 2 mg/kg/day via intraperitoneal injection for 5 consecutive days (days 1–5) (22, 23). No eugenol or eugenol solvent was administered to this group during days 6–15.

5- Paclitaxel + Eugenol 5 group (PTX+EUG5): Animals received paclitaxel (2 mg/kg/day, IP) for 5 days (days 1–5), followed by eugenol at a dose of 5 mg/kg/day via oral gavage for 10 days (days 6–15).

6- Paclitaxel + Eugenol 25 group (PTX+EUG25): Animals received paclitaxel (2 mg/kg/day, IP) for 5 days (days 1–5), followed by eugenol at a dose of 25 mg/kg/day via oral gavage for 10 days (days 6–15) (12, 13).

Preparation and administration of eugenol

Eugenol (Sigma-Aldrich, E51791) was freshly prepared daily by dissolving it in physiological saline (0.9% NaCl) to achieve a final concentration of 1 mg/100 µl. The solution was gently mixed immediately before oral gavage.

Blood pressure parameters evaluation

Noninvasive tail-cuff blood pressure measurements were performed in rats using a volume-pressure recording method (MAY-NIBP250, Türkiye). Cuffs were routinely checked for patency before experiments. Animals were habituated to the restraint and tail-cuff procedure for 7 consecutive days. All measurements were conducted in a designated quiet area (22 ± 2 °C), and rats were acclimatized for 1 hr prior to recording to minimize stress-related sympathetic activation. Animals were gently guided into restraint tubes to minimize movement. The occlusion cuff was placed at the base of the tail, and the sensor cuff was positioned adjacent to it. A heating chamber maintained at 32 °C was used, and rats were warmed for 5 min before and during recordings. Blood pressure was measured by inflating the occlusion cuff to 250 mmHg and deflating it over 15 sec, while the sensor cuff detected volume changes in the tail. Rats were habituated for at least 7 consecutive days before baseline measurements. For each animal, five measurements were taken at 1-min intervals. The highest and lowest values were excluded, and the mean of the remaining three measurements was used to obtain systolic pressure, diastolic

pressure, heart rate, and mean arterial pressure data. Mean arterial pressure was calculated using the formula: Mean Arterial Pressure = Diastolic Pressure + (Systolic Pressure – Diastolic Pressure)/3. MAP was calculated using the formula: MAP = DBP + (SBP - DBP) / 3 (24).

Serum biomarker analysis (cTnT and BNP) analysis

On the 16th day of the study, animals were deeply anesthetized with xylazine (10 mg/kg, IP) and ketamine (60 mg/kg, IP). Adequate depth of anesthesia was confirmed by the absence of withdrawal and corneal reflexes. After confirming surgical anesthesia, cardiac blood samples were collected, after which animals were euthanized and the hearts were rapidly excised for further analyses. The collected blood in tubes was allowed to stand for 30 min and then centrifuged at 3000 rpm for 10 min. Non-hemolyzed serum samples were aspirated into an Eppendorf tube and kept at -80 °C until needed for biochemical testing. The ELISA technique was used to measure cardiac troponin T (cTnT) (Finetest Lot no: ER1396) and brain natriuretic peptide (BNP) (Finetest ER0775) levels (24).

Histopathological analysis

The heart tissues were fixed in 10% neutral formalin for 72 hr, treated with ethanol, and then embedded in paraffin blocks for histological examinations. Sections 6 µm thick were cut from a paraffin block (Leica, Autocut, 14051956472, Germany) and stained with hematoxylin and eosin (H&E) (Bio-Optica 05-06004/L Harris' Hematoxylin & Bio-Optica 05-10002/L, Eosin Y %1) and with iron hematoxylin to examine the general histomorphological structure of heart tissues. Standard light microscopy (Nikon, Eclipse Ni-U, 940728, equipped with a camera) was used to analyze heart tissue under blinded conditions. Histopathological alterations were semi-quantitatively scored for myocardial degeneration, cardiomyocyte hypertrophy, edema, nuclear damage (pyknosis/karyolysis), myofibrillar disorganization and vacuolization. Each parameter was graded on a scale from 0 (absent) to 3 (severe) in 15 randomly selected fields per section by a blinded observer. The total histopathological injury score was calculated by summing individual parameter scores (24, 25).

Hematoxylin and eosin (H&E) staining was used for general histopathological evaluation of myocardial injury, including edema, hemorrhage, cellular degeneration, and nuclear alterations (25). Iron hematoxylin staining was also used to assess myofibrillar organization, actin–myosin striation patterns, and cardiomyocyte structural integrity (24).

Immunohistochemistry

The immunohistochemical staining kit (Lab VisionTM UltraVisionTM Large Volume Detection System: anti-polyvalent, HRP, TA-125-HL) was used in conjunction with the streptavidin-biotin-peroxidase method. This method was used to assess the expression of mTOR, ULK1, and Atg13 in heart tissue. Five-micron-thick cross-sections of heart tissue blocks were cut, deparaffinized, rehydrated, and washed at room temperature in phosphate-buffered saline (PBS). To prevent endogenous peroxidase activity, 3% hydrogen peroxide was applied for 5 min. They were rewashed with PBS and incubated in 10% sodium citrate buffer (pH 6.0) for 10 min at 600W in a microwave oven. They were subsequently allowed to rest at room temperature for 20 min and then washed with phosphate-buffered saline (PBS). To inhibit endogenous peroxidase activity, a hydrogen peroxide solution was applied for 10 min. After washing the tissues with PBS, a blocking solution was applied for 10 min. Primary antibodies mTOR (Proteintech, Cat No. 66888-1-Ig, 1/1000), ULK1 (Proteintech, Cat No. 20986-1-AP, 1:100), Atg13 (Proteintech; Cat No. 18258-1-AP, 1:250), were treated with the sections for an over night at 4 °C. After incubation, the tissues were washed with PBS, followed by a 30-min incubation with a secondary antibody compatible with the primary antibody. Finally, the tissues were washed again with PBS and incubated with Streptavidin Peroxidase (Thermo Scientific SHRP248-B) for 20 min at room temperature in a humidified chamber, and then placed in PBS. After applying Diaminobenzidine (DAB) solution, the tissues were observed under a light microscope until the signal was detected, followed by simultaneous washing of all groups with tap water. The sections were counterstained with Mayer's hematoxylin, passed through PBS and distilled water, and then mounted with an appropriate mounting solution. The immunohistochemically stained sections were examined using a light microscope (Nikon Eclipse Ni-U, 940728), and images were captured from 20 randomly selected fields per section. Immunoreactivity intensities of mTOR, ULK1, and Atg13 were quantified using ImageJ (NIH, Bethesda, MD, USA), and the resulting data were used for statistical analysis (25, 26).

Statistical analyses

The results of the analyses were evaluated using GraphPad Prism 9.0. The Shapiro-Wilk test was performed to assess the normality of the data distribution. For comparisons involving multiple groups, one-way analysis of variance (ANOVA) and the Kruskal-Wallis test were utilized. *Post hoc* analyses were conducted using the Bonferroni test for ANOVA and the Dunn's multiple comparisons test for the Kruskal-Wallis test. A *P*-value below 0.05 was considered statistically significant for all analyses.

Results

Evaluation of systolic and diastolic blood pressure

After all treatments were completed, systolic blood pressure (SBP) and diastolic blood pressure (DBP) were measured in the experimental groups. The PTX group ($P<0.05$) and the EUG25 group ($P<0.01$) showed significantly lower SBP values than the control group. However, the EUG5 group had significantly higher SBP values than the EUG25 group ($P<0.01$). Although PTX administration reduced SBP relative to the control group, no significant changes were observed in the PTX groups treated with either EUG5 or EUG25 (Figure 2a). Similarly, the PTX group exhibited significantly lower DBP values than the control group ($P<0.01$). Although PTX treatment decreased DBP, the PTX groups that received EUG (EUG5 or EUG25) showed no significant changes in DBP (Figure 2b).

Evaluation of mean arterial blood pressure and heart rate

Following completion of all experimental procedures, mean arterial pressure (MAP) and heart rate were measured across all study groups. PTX administration significantly decreased MAP values compared to the control group ($P<0.001$). Both PTX+EUG5 and PTX+EUG25 treatment groups showed significantly higher MAP values than the PTX group ($P<0.05$), though no significant difference was observed between these two treatment groups (Figure 2c). Regarding heart rate measurements, the PTX group showed

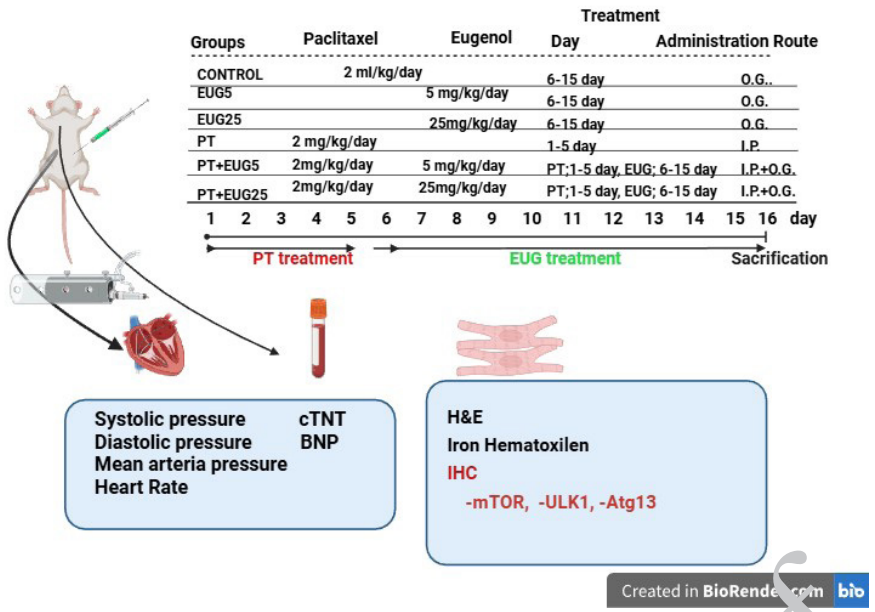

Figure 1. Schematic representation of the experimental design
IP: Intraperitoneal administration, cTnT: Cardiac troponin T, BNP: Brain Natriuretic Peptide; mTOR: Mechanistic target of rapamycin; ULK1: Unc-51 like autophagy activating kinase 1; Atg13: Autophagy-related protein 13; H&E: Hematoxylin and eosin; IHC: Immunohistochemical staining

significantly lower values than controls (P<0.01). While the EUG25 group demonstrated a significant increase in heart rate relative to the PTX group (P<0.001), the PTX+EUG5 and PTX+EUG25 groups showed non-significant increases in heart rate compared to PTX treatment (Figure 2d).

Compared with the PTX group, PTX+EUG5 showed a 18.9% increase in MAP, and PTX+EUG25 showed a 19.3% increase, indicating significant recovery toward normal hemodynamic values. These results suggest that EUG may attenuate PTX-induced hypotension in a dose-responsive manner, with higher doses of EUG25 providing marginally greater restoration of MAP than lower doses of EUG5.

Assessment of serum cTnT and BNP levels

cTnT and BNP levels were assessed following all experimental applications. PTX administration significantly increased both cTnT and BNP levels compared to the control group (P<0.001). In contrast, EUG treatment significantly reduced these cardiac injury markers. In the PTX+EUG5 and PTX+EUG25 groups, cTnT levels were significantly lower than those in the PTX group (P=0.021 and P<0.001, respectively), while BNP levels were also markedly reduced in both groups (P<0.001). Compared with the PTX group, both EUG-treated groups showed reductions in cardiac injury biomarkers. PTX+EUG5 was associated with a 10.02% decrease in cTnT and a 32.99% decrease in BNP levels, while PTX+EUG25 resulted in reductions of 17.18% and 37.67%, respectively (Figure 3a–b).

Interestingly, cTnT and BNP levels in the EUG-only groups were lower than those observed in the control group. Although this finding may appear unexpected under physiological conditions, it likely reflects the potent antioxidant and anti-inflammatory properties of EUG, which may reduce basal oxidative and inflammatory tone even in healthy myocardium. Importantly, this reduction should not be interpreted as an improvement in cardiac function, but rather as a biochemical modulation within physiological limits, as no functional cardiac assessments were performed in the present study.

Histomorphological analysis

H&E staining

H&E-stained heart sections from the control and EUG-

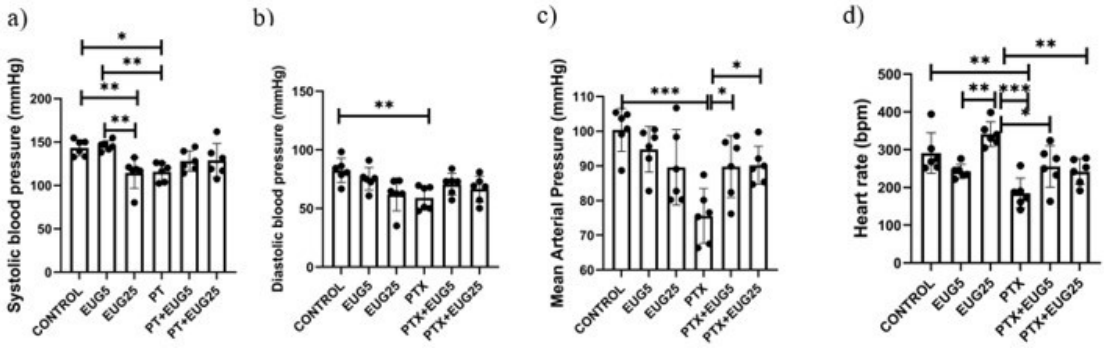

Figure 2. Levels of blood pressure parameters in rat control and treated groups in paclitaxel (PTX) toxicity
Data are presented as mean ± SD (n = 6 per group; biological replicates). Blood pressure was measured five times per animal; the highest and lowest values were excluded, and the average of the remaining three values was calculated for each animal. a) Comparison of systolic blood pressure among study groups in PTX-induced toxicity. Data are represented as mean±standart deviation. b) Comparison of diastolic blood pressure among study groups in PTX-induced toxicity. Data are represented as mean±standart deviation. c) Comparison of mean arterial pressure among study groups in PTX-induced toxicity. d) Comparison of heart rate among study groups in PTX-induced toxicity.
Data are represented as mean±standart deviation and the statistical differences were analyzed by one-way ANOVA. * <0.05 , ** <0.01 , ***<0.001. EUG: Eugenol; PT: ???

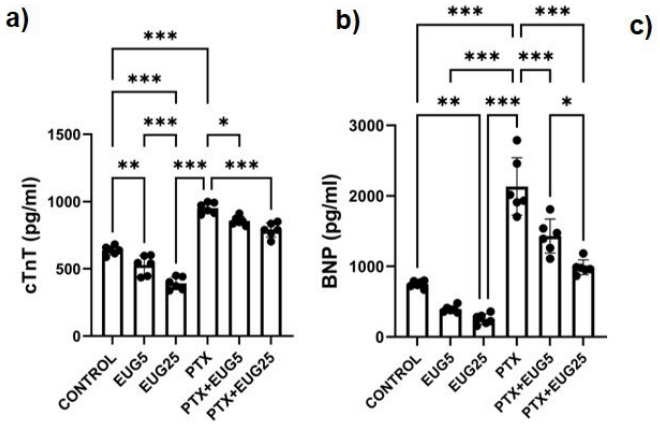

Experimental groups	c-TnT levels (mean±SD)	BNP levels (mean±SD)
CONTROL	637,1 ± 33,14	748,4 ± 49,85
PT	952,4 ± 40,93	2134 ± 406,2
EUG5	527,7 ± 71,98	393,4 ± 47,29
EUG25	391,6 ± 47,28	252,5 ± 73,62
PT+EUG5	857,0 ± 33,20	1430 ± 240,8
PT+EUG25	788,8 ± 52,62	988,7 ± 105,0

Figure 3. Serum cardiac troponin T (cTnT) and brain natriuretic peptide (BNP) levels in control and rat experimental groups following paclitaxel (PTX) administration and eugenol (EUG) treatment

Data are presented as mean ± SD (n = 6 rats per group; three technical replicates per sample). Statistical analysis was performed using one-way ANOVA. **P*<0.05, ***P*<0.01, ****P*<0.001.

only groups exhibited a largely preserved myocardial architecture, characterized by normal cardiomyocytes with centrally located nuclei. Mild interstitial edema was occasionally observed in the EUG25 group. In contrast, heart tissues from the PTX group showed pronounced histopathological alterations, including cardiomyocyte degeneration and hypertrophy, interstitial edema, hemorrhage, pyknotic nuclei, and vacuole formation between cardiomyocytes.

In the PTX+EUG25 group, PTX-induced histopathological changes were markedly attenuated. The myocardial architecture in this group was largely preserved and closely resembled that of the control and EUG5 groups. In the PTX+EUG5 group, a partial protective effect was observed, with reduced hemorrhage, edema, and cardiomyocyte hypertrophy compared with the PTX group (Figure 4).

Iron hematoxylin staining

Iron hematoxylin–stained sections from the control group demonstrated well-preserved actin–myosin striations and normal nuclear morphology. In contrast, cardiomyocytes in the PTX group exhibited hypertrophy, karyolytic and pyknotic nuclei, and a marked loss of myofibrillar striations, indicating disruption of actin–myosin organization. Prominent interstitial edema was also evident in this group.

In the PTX+EUG treatment groups, particularly PTX+EUG25, these ultrastructural alterations were substantially attenuated. Cardiomyocytes showed preserved nuclear morphology, clearer myofibrillar striations, and reduced interstitial edema, indicating partial restoration of myofibrillar organization following EUG treatment (Figure 5).

Histopathological scoring of myocardial injury

Semi-quantitative histopathological scoring based on hematoxylin and eosin (H&E) staining revealed marked myocardial injury in the PTX group, characterized by significantly higher scores for cardiomyocyte degeneration/hypertrophy, edema, hemorrhage, vacuolization, nuclear damage, and myofibrillar disorganization compared with the control and EUG-only groups ($P<0.05$).

Evaluation of iron hematoxylin–stained sections further confirmed severe myocardial structural disorganization in the PTX group, particularly with respect to nuclear damage and myofibrillar integrity.

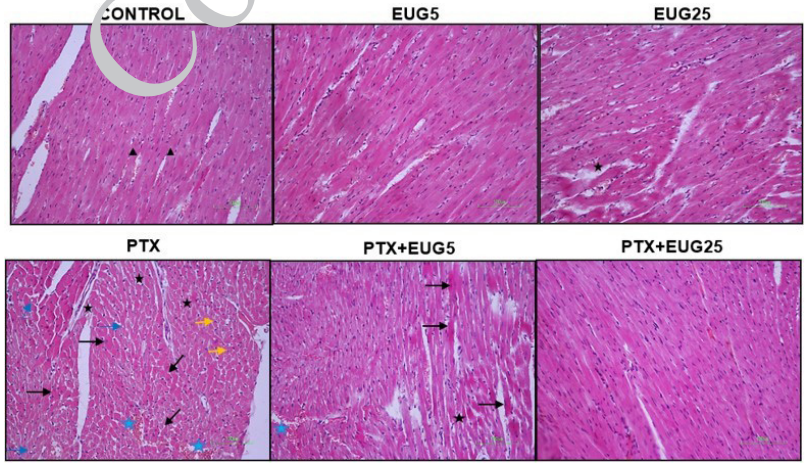

Figure 4. Histopathological assessment of PTX-induced myocardial injury and its modulation by eugenol treatment in rats. Cardiac tissue sections (n = 6 per group) stained with Hematoxylin and Eosin (H&E) were analyzed at ×200 magnification (Nikon Eclipse Si, Tokyo, Japan). Scale bar: 100 µm

The control and EUG groups exhibit normally branched and anastomosed cardiomyocytes with centrally located oval nuclei (triangle). In contrast, the PTX group displays hemorrhage between cardiomyocytes (blue star), interstitial edema (black star), pyknotic nuclei (yellow arrow), hypertrophic fibrils (black arrow), and vacuoles (blue arrow). In the PTX+EUG5 group, reduced hemorrhage, edema, and hypertrophic fibrils were observed, whereas the PTX+EUG25 group showed a histological appearance closer to that of the control group.

EUG: Eugenol; PTX: Paclitaxel

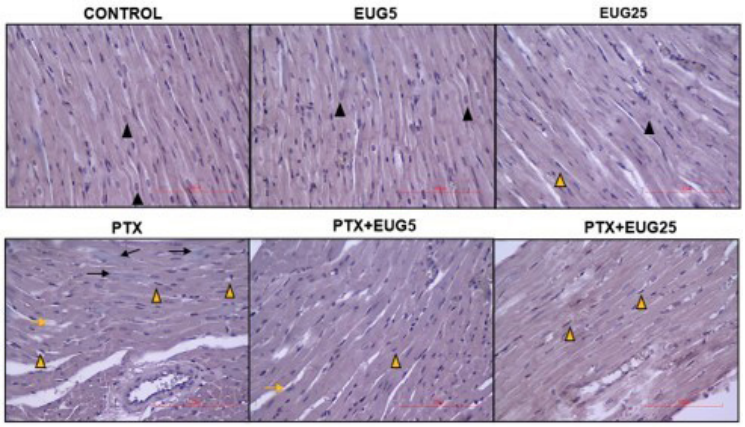

Figure 5. Histological analysis of rat heart..... sections (n = 6 per group) stained with İron-Hematoxylin at ×200 magnification (Nikon Eclipse Si, Tokyo, Japan; scale bar: 100 µm)
The control and EUG groups exhibit normal histoarchitecture, with centrally located oval nuclei (black arrowhead) and striated muscle fibers. In the PTX group, hypertrophic myocardial fibers with large and irregular shapes are observed, along with karyolytic nuclei (black arrow), pyknotic nuclei (yellow arrowhead), and interstitial edema (yellow arrow).

In contrast, rats treated with eugenol after PTX exposure exhibited significantly lower histopathological scores in both H&E and iron-hematoxylin assessments. Both PTX+EUG5 and PTX+EUG25 groups showed a substantial reduction in myocardial edema, vacuolization, nuclear damage, and myofibrillar disorganization compared with the PTX group (P<0.05).

No significant histopathological differences were observed between the control and EUG-only groups under either staining modality, whereas the myocardial histoarchitecture of the PTX+EUG25 group was largely comparable to that of the control group across most evaluated parameters (Table 1).

Immunohistochemical analysis

The IHC staining images of heart tissue are presented in Figure 6, while the immunoreactivity results are shown in Figure 7. mTOR is a protein that inhibits autophagy by phosphorylating ULK1. Therefore, its expression was more intense in the control group. In the PTX group, a decrease in mTOR expression was detected, whereas an increase in expression was observed in the PTX+EUG5 and PTX+EUG25 groups following EUG administration. ULK1 and Atg13, which play critical roles in autophagy activation, showed low expression levels in the control group. However, in the PTX group, these proteins showed more intense staining. In the PTX+EUG5 and PTX+EUG25 groups, the intensity of ULK1 and Atg13 expression was reduced (Figure 6).

Induction of the autophagic process by PTX administration led to a significant decrease in mTOR

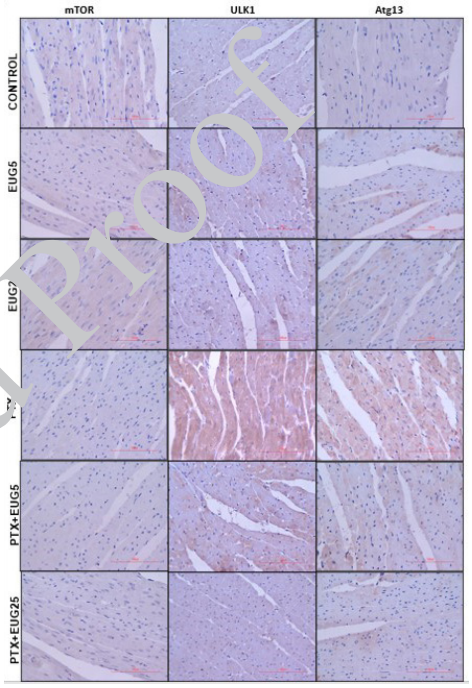

Figure 6. Immunohistochemical analysis of rat heart sections (n = 6 per group) (Nikon Eclipse Si, Tokyo, Japan. X400: Scale bar; 100 µm)
Levels of autophagy markers in the hearts of the control and treated groups. EUG treatment modulated the expression of mTOR, ULK1, and Atg13 in the hearts of PTX-treated rats. Avidin-biotin peroxidase technique.
mTOR: Mammalian target of rapamycin; ULK1: Unc-51-like kinase, Atg13: Autophagy-related protein 13; EUG: Eugenol; PTX: Paclitaxel

Table 1. Semi-quantitative histopathological scoring of rat myocardial injury

Myocardial Injury Histoscorring (0–3)	Control	EUG5	EUG25	PTX	PTX+EUG5	PTX+EUG25
H&E staining (general myocardial injury parameters)						
Cardiomyocyte degeneration/hypertrophy	0 [0–0]^{a}	0 [0–0]^{a}	0 [0–0]^{a}	2 [2–3]^{c}	1 [0.5–2]^{b}	1 [0–1.5]^{b}
Edema	0 [0–1]^{a}	0 [0–1]^{a}	0 [0–1]^{a}	3 [1–3]^{c}	2 [0–3]^{b}	1 [0–3]^{b}
Hemorrhage	0 [0–1]^{a}	0 [0–1]^{a}	0 [0–2]^{a}	3 [1–3]^{c}	2 [0–3]^{b}	1 [0–2]^{b}
Vacuolization	0 [0–1]^{a}	0 [0–1]^{a}	0 [0–1]^{a}	2 [1–3]^{c}	1 [0–2]^{b}	1 [0–2]^{b}
Iron hematoxylin staining (myofibrillar and nuclear integrity)						
Nuclear damage	0 [0–1]^{a}	0 [0–1]^{a}	0 [0–1]^{a}	3 [1–3]^{c}	2 [0–2]^{b}	1 [0–2]^{b}
Myofibrillar disorganization	0 [0–1]^{a}	0 [0–1]^{a}	0 [0–1]^{a}	3 [2–3]^{c}	1 [0–2]^{b}	1 [0–1]^{b}

Data are expressed as median [min–max]. Histopathological scoring was performed separately for H&E and iron-hematoxylin-stained sections. Statistical analysis was performed using the Kruskal–Wallis test followed by Dunn's post hoc test. Different superscript letters (a–c) indicate statistically significant differences between groups within the same staining modality and parameter; groups sharing the same letter are not significantly different from each other, whereas groups with different letters differ significantly (P<0.05). EUG: Eugenol; PTX: Paclitaxel

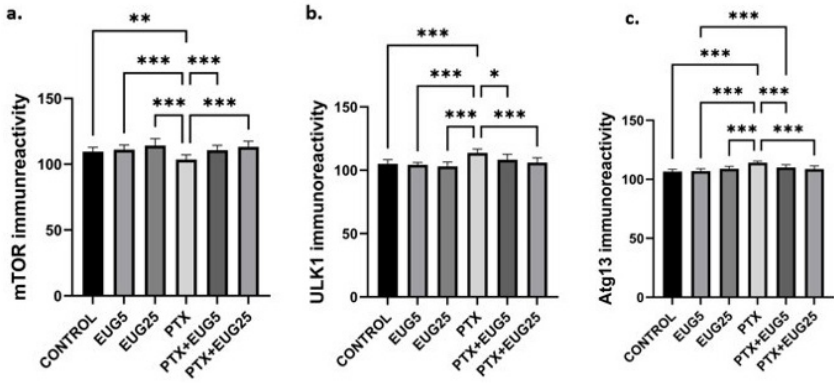

Figure 7. Immunoreactivity intensity of rat autophagy proteins
Impact of EUG mTOR, ULK1, and Atg13 in the heart tissue of rats treated with PTX. Data are represented as mean±SD (n = 6 per group. For each animal, more than 20 representative images were analyzed) and the statistical differences were analyzed by one-way ANOVA. *<0.05, **<0.01, ***<0.001.
EUG: Eugenol; PTX: Paclitaxel; mTOR: Mammalian target of rapamycin; ULK1: Unc-51-like kinase,

expression, which was highly expressed in the control group (P<0.01). In the EUG5 and EUG25 groups, mTOR expression was relatively high compared to control; however, in the PTX+EUG5 and PTX+EUG25 groups, where PTX was administered followed by treatment, a significant increase in mTOR expression was observed (P<0.001) (Figure 7a). The autophagy-related proteins ULK1 and Atg13 showed a significant increase in expression in the PTX group compared to the control group (P<0.001). ULK1 expression was significantly reduced in the PTX+EUG5 (P<0.05) and PTX+EUG25 groups (P<0.001) (Figure 7b). Similarly, Atg13 expression showed a significant decrease in the PTX+EUG5 and PTX+EUG25 (P<0.001) groups (Figure 7c).

Discussion

In the present study, PTX administration resulted in marked myocardial injury, as evidenced by elevated biochemical injury markers and pronounced histopathological alterations in cardiac tissue. These findings indicate that PTX exposure is associated with stress-related myocardial damage rather than primary impairment of cardiac function. The observed structural changes and tissue injury patterns are consistent with pathological processes commonly linked to oxidative stress and inflammatory activation, as reported in previous studies.

Treatment with EUG significantly attenuated PTX-induced myocardial injury, as reflected by reduced histopathological scores and improvements in biochemical parameters. These protective effects may be attributed to EUG's known xidant and anti-inflammatory properties, which have been shown to mitigate cellular stress and structural damage in cardiac tissue. Importantly, the reductions observed in injury markers and histopathological scores in the EUG-treated groups represent attenuation of myocardial injury rather than restoration of cardiac function, which was not directly assessed in this study. Although the higher EUG dose demonstrated more pronounced protective effects in some parameters, the overall findings do not indicate a consistent dose-dependent response across all evaluated outcomes.

PTX is a highly effective chemotherapeutic agent, but its clinical use is limited by cardiotoxic effects resulting from microtubule disruption, oxidative stress, and altered cardiomyocyte signaling (27). Although some studies have reported preserved hemodynamic parameters following PTX exposure, these findings are often accompanied by subclinical myocardial or autonomic alterations rather than overt cardiac dysfunction (28, 29). In this context, the reductions in arterial blood pressure and heart rate observed in the present study may reflect disturbances in cardiovascular regulation induced by PTX. The partial attenuation of these changes by EUG suggests a modulatory effect on PTX-related cardiovascular stress, likely mediated by its xidant and anti-inflammatory properties. However, in the absence of direct functional assessments, these findings should be interpreted as indicative of physiological regulation rather than definitive functional recovery.

Consistent with this cautious interpretation, EUG treatment following PTX exposure significantly influenced only arterial blood pressure parameters in the present study, whereas heart rate remained largely unaffected. This limited hemodynamic response contrasts with reports of broader cardiovascular effects of EUG observed in non-PTX experimental settings, suggesting that the therapeutic efficacy of EUG in PTX-induced cardiac injury may depend on the underlying mechanism of injury and the duration of treatment. Importantly, PTX-induced cardiotoxicity is strongly associated with microtubule-stabilization–dependent disturbances in intracellular Ca^{2+} signaling, including enhanced spontaneous Ca^{2+} oscillations mediated by NCS-1 and $InsP_3$ receptor interactions (4, 30). In this context, the modest cardiovascular improvement observed with short-term EUG administration may reflect partial modulation of PTX-induced oxidative and Ca^{2+}-dependent stress rather than full restoration of cardiac autonomic or contractile function. Consistent with recent evidence highlighting the role of EUG in attenuating chemotherapy-related oxidative and calcium-mediated myocardial stress (31), prolonged EUG exposure may be required to counteract PTX-driven intracellular Ca^{2+} dysregulation and its downstream cardiovascular consequences.

Troponin T and BNP are well-recognized early biomarkers of cardiotoxicity and myocardial stress (3). In the present study, PTX administration significantly increased both cTnT and BNP levels, confirming PTX-induced myocardial injury. In contrast, EUG treatment administered after PTX exposure significantly reduced these biomarkers in both PTX+EUG groups. Although cTnT levels did not differ significantly between EUG doses, BNP levels were significantly lower in the PTX+EUG25 group than in the PTX+EUG5 group, suggesting a more pronounced effect of the higher dose on ventricular stress–related biochemical

signaling rather than a uniform dose-dependent response.

The observed reduction in cardiac biomarkers is likely related to EUG's established cardiovascular actions. EUG has been shown to lower systemic blood pressure by endothelium-dependent vasorelaxation, mediated by TRPV4 channel activation and inhibition of voltage-dependent Ca^{2+} influx, thereby reducing myocardial workload (32, 33). When administered following established PTX-induced injury, these hemodynamic and cellular effects may attenuate ongoing myocardial stress and limit further cardiomyocyte damage, resulting in reduced circulating levels of cTnT and BNP. Consistent with previous reports describing PTX-induced elevations in cardiac injury biomarkers (27) and evidence supporting the ability of EUG to ameliorate biochemical indicators of cardiotoxicity (31–33), the present findings support a therapeutic rather than prophylactic role of EUG in mitigating PTX-induced myocardial injury at the biochemical level, without implying full restoration of cardiac function.

PTX, a microtubule stabilizer, is known to induce myocardial histopathological alterations, including cardiomyocyte degeneration, edema, hemorrhage, and structural disorganization (24, 34). Consistent with these reports, our histopathological scoring showed severe myocardial injury in the PTX group, characterized by increased edema, hemorrhage, nuclear damage, vacuolization, and myofibrillar disorganization.

In contrast, EUG treatment markedly attenuated PTX-induced myocardial structural damage, as reflected by significantly reduced histopathological injury scores in both PTX+EUG groups, with near-normal histoarchitectural features observed at the higher dose. These findings suggest that EUG does not merely reverse established tissue damage but rather limits early stress-mediated structural disruption initiated by PTX. PTX-induced cardiotoxicity is known to involve oxidative stress, inflammatory activation, and mitochondrial dysfunction, which collectively contribute to cardiomyocyte degeneration and interstitial disorganization. In line with this mechanism, xidant-based interventions have been shown to preserve myocardial histological integrity in PTX-treated experimental models by interrupting oxidative and inflammatory injury cascades. Previous studies have demonstrated that EUG effectively suppresses inflammatory signaling and oxidative damage in cardiac tissue (12, 14, 31), while recent PTX-specific models report comparable histopathological protection with agents such as melatonin, resveratrol, and misoprostol (34–36). Collectively, these data indicate that EUG exerts a therapeutic injury-attenuating effect at the histological level by constraining PTX-driven myocardial stress and structural injury, rather than restoring overt cardiac function.

Under cellular stress conditions, autophagy is rapidly activated as an adaptive response, with an early increase in autophagic flux occurring within min to hours, followed by a more sustained transcriptionally regulated phase mediated by autophagy-related genes (25). Energy stress–induced inhibition of mTOR is a central trigger for this process, facilitating the activation of ULK1, a key initiator of mammalian autophagy. ULK1 functions by forming a multiprotein complex with Atg13, Atg101, and FIP200, thereby initiating autophagosome formation under stress conditions (37, 38). In the present study, PTX exposure was associated with suppression of mTOR expression accompanied by increased ULK1 and Atg13 immunoreactivity, suggesting a shift toward stress-driven autophagy initiation rather than a balanced cytoprotective response. Excessive or dysregulated autophagy has been implicated in chemotherapy-induced cardiomyocyte injury. Notably, post-treatment with EUG, particularly at the higher dose, partially restored mTOR expression while reducing ULK1 and Atg13 levels, indicating modulation of early autophagy signaling. These findings suggest that EUG does not abolish autophagy but may recalibrate the mTOR–ULK1–Atg13 axis toward a more controlled cellular stress response, thereby limiting autophagy-associated myocardial injury under PTX-induced cardiac stress.

Conclusion

This study demonstrates that EUG attenuates PTX-induced cardiac injury in a rat model. Post-treatment with EUG, particularly at 25 mg/kg, reduced histopathological damage and improved biochemical markers of myocardial injury, including decreased circulating cTnT and BNP levels, and partially normalized arterial blood pressure parameters. Mechanistically, these effects appear to be associated with modulation of autophagy-related signaling, involving regulation of the mTOR/ULK1/Atg13 axis, in parallel with EUG's established xidant and anti-inflammatory properties. Although further studies are required to comprehensively assess autophagic flux and long-term functional outcomes, the present findings suggest that EUG may exert a therapeutic, injury-attenuating effect in chemotherapy-induced cardiac damage and support its potential role as an adjunctive strategy to limit PTX-associated cardiotoxicity.

Acknowledgment

The Experimental and the Clinical Research Center at Kırşehir Ahi Evran University, Türkiye, provided laboratory facilities and technical support for this investigation, which the authors gratefully acknowledge.

Limitation and Future Perspectives

Several limitations of this study should be acknowledged. First, although the therapeutic effects of EUG (5 and 25 mg/kg) were evaluated during the subacute phase of PTX-induced cardiac injury, longer-term outcomes and potential cumulative effects were beyond the scope of the present design. Second, the exclusive use of male rats and reliance on a noninvasive tail-cuff method for blood pressure assessment may limit the generalizability and resolution of hemodynamic measurements; however, this approach was supported by rigorous animal habituation and standardized measurement protocols. Third, the treatment groups were not fully matched in handling procedures and vehicle administration, as the PTX solvent was not administered to all groups during the initial phase, and the eugenol vehicle was not given during the subsequent phase; therefore, the potential confounding effects of repeated oral gavage stress or vehicle exposure could not be fully controlled. Importantly, although our findings indicate modulation of the mTOR/ULK1/Atg13 signaling axis, the absence of direct autophagic flux assessments (such as LC3-II and p62 turnover) and ultrastructural confirmation precludes definitive conclusions regarding dynamic autophagy activity. Future studies incorporating both sexes, extended treatment periods, invasive hemodynamic monitoring, and comprehensive autophagic flux analyses will be valuable for further strengthening the mechanistic understanding and

translational relevance of EUG.

Funding

The authors did not receive support from any organization for the submitted work.

Authors' Contributions

S KG, O K, and MN B designed the experiments; H TY, S KG, and SK performed the experiments and collected the data; H TY and SK discussed the results and strategy; S KG, MNB supervised, directed, and managed the study; H TY, S KG, O K, S K, and MN B approved the final version for publication.

Conflicts of Interest

The authors declare that they have no known competing financial interests or personal relationships that could have appeared to influence the work reported in this paper.

Declaration

We acknowledge the use of AI-assisted language editing tools solely for grammar and language improvement. The scientific content, data analysis, interpretation, and conclusions are entirely the responsibility of the authors.

References

1. Zhu L, Chen L. Progress in research on paclitaxel and tumor immunotherapy. Cell Mol Biol Lett 2019; 24:40.
2. Yu DL, Lou ZP, Ma FY, Najafi M. The interactions of paclitaxel with tumour microenvironment. Int Immunopharmacol 2022; 105:108555.
3. Bertolini D, Pizzi C, Donal E, Galli E. Cancer and heart failure: Dangerous liaisons. J Cardiovasc Dev Dis 2024; 11:263.
4. Zhang K, Heidrich FM, DeGray B, Boehmerle W, Ehrlich BE. Paclitaxel accelerates spontaneous calcium oscillations in cardiomyocytes by interacting with NCS-1 and the InsP3R. J Mol Cell Cardiol 2010; 49: 829–835.
5. Nagy A, Börzsei D, Hoffmann A, Török S, Veszela M, Annasi N *et al.* A comprehensive overview on chemotherapy-induced cardiotoxicity: Insights into the underlying inflammatory and oxidative mechanisms. Cardiovasc Drugs Ther 2024. doi:10.1007/s10557-024-07574-0.
6. Zhang J, Xiang Q, Wu M, Lao YZ, Xian YF, Xu HX *et al.* Autophagy regulators in cancer. Int J Mol Sci 2023; 24:10944.
7. Harborne JB, Baxter H. Phytochemical Dictionary. London: Taylor & Francis; 1993.
8. Özarslan M, Avcıoğlu NH, Can DP, Çalışkan A. Biofilm formation of Candida albicans on occlusal device materials and antibiofilm effects of chitosan and eugenol. J Prosthet Dent 2024; 131:144.e1–144.e7.
9. Barot J, Saxena B. Therapeutic effects of eugenol in a rat model of traumatic brain injury: A behavioral, biochemical, and histological study. J Tradit Complement Med 2021; 11:318–327.
10. Miyazawa M, Hisama M. Suppression of chemical mutagen-induced SOS response by alkylphenols from clove (Syzygium aromaticum) in Salmonella typhimurium TA1535/pSK1002 umu test. J Agric Food Chem 2001; 49:4019–4025.
11. Pramod K, Ansari SH, Ali J. Eugenol: A natural compound with versatile pharmacological actions. Nat Prod Commun 2010; 5:1999–2006.
12. Damasceno ROS, Pinheiro JLS, Rodrigues LHM, Gomes RC, Duarte ABS, Emídio JJ, *et al.* Anti-inflammatory and anti-oxidant activities of eugenol: An update. Pharmaceuticals (Basel) 2024; 17:1505.
13. Fathy M, Abdel-Latif R, Abdelgwad YM, Othman OA, Abdel-Razik AH, Dandekar T, *et al.* Nephroprotective potential of eugenol in a rat experimental model of chronic kidney injury: Targeting NOX, TGF-β, and Akt signaling. Life Sci 2022; 308:120957.
14. Feng W, Jin L, Xie Q, Huang L, Jiang Z, Ji Y *et al.* Eugenol protects the transplanted heart against ischemia/reperfusion injury in rats by inhibiting the inflammatory response and apoptosis. Exp Ther Med 2018; 16:3464–3470.
15. Filomeni G, De Zio D, Cecconi F. Oxidative stress and autophagy: The clash between damage and metabolic needs. Cell Death Differ 2015; 22:377–388.
16. Kaarniranta K, Blasiak J, Liton P, Boulton M, Klionsky DJ, Sinha D. Autophagy in age-related macular degeneration. Autophagy 2023; 19:388–400.
17. Liu GY, Sabatini DM. mTOR at the nexus of nutrition, growth, ageing and disease. Nat Rev Mol Cell Biol 2020; 21:183–203.
18. Kim J, Kundu M, Viollet B, Guan KL. AMPK and mTOR regulate autophagy through direct phosphorylation of ULK1. Nat Cell Biol 2011; 13:132–141.
19. Zhang X, Zhang H, Gao Y, Hao Z, Liu J, Zhou G *et al.* Forsythoside A regulates autophagy and apoptosis through the AMPK/mTOR/ULK1 pathway and alleviates inflammatory damage in MAC-T cells. Int Immunopharmacol 2023; 118:110053.
20. Shaernejad S, Nosrat A, Baeeri M, Goradel NH, SeyedSadeghi M, Akbairani M *et al.* Role of hesperidin/hesperetin against chemotherapy-induced cardiotoxicity: A systematic review of nonclinical studies. Cancer Cell Int 2025; 25:1–13.
21. Devi S, Chauhan S, Mannan A, Singh TG. Targeting cardiovascular risk factors with eugenol: An anti-inflammatory perspective. Inflammopharmacology 2024; 32:307–317.
22. Yakut S, Atcalı T, Çağlayan C, Ulucan A, Kandemir FM, Kara A *et al.* Therapeutic potential of silymarin in mitigating paclitaxel-induced hepatotoxicity and nephrotoxicity: Insights into oxidative stress, inflammation, and apoptosis in rats. Balkan Med J 2024; 41:198–204.
23. Serin HS, Kandemir FM, Kaynar O, Dogan T, Arikan SM. The protective effects of hesperidin against paclitaxel-induced peripheral neuropathy in rats. Life Sci 2021; 287:120104.
24. Koçak S, Kalkan KT, Aydın ÖS, Öztürk K. Cardioprotective effects of carvacrol in the isoproterenol-induced myocardial infarction model. BMC Pharmacol Toxicol 2025; 26:132.
25. Aly E, El-Mashad ABI, Tantawy AA, Amin AA. A comparative study on the cardiopulmonary protective effect of propolis versus coenzyme Q10 on paclitaxel-induced toxicity. J Adv Vet Res 2023; 14:59–64.
26. Ruifrok AC, Johnston DA. Quantification of histochemical staining by color deconvolution. Anal Quant Cytol Histol 2001; 23:291–299.
27. Joshi AM, Prousi GS, Bianco C, Malla M, Guha A, Shah M *et al.* Microtubule inhibitors and cardiotoxicity. Curr Oncol Rep 2021; 23:30.
28. Ekholm E, Rantanen V, Antila K, Salminen E. Paclitaxel changes sympathetic control of blood pressure. Eur J Cancer 1997; 33:1419–1424.
29. Altin C, Sade LE, Demirtas S, Karacaglar E, Kanyilmaz S, Simsek V *et al.* Effects of paclitaxel and carboplatin combination on mechanical myocardial and microvascular functions: A transthoracic Doppler echocardiography and two-dimensional strain imaging study. Echocardiography 2015; 32:238–247.
30. Rowinsky EK, McGuire WP, Guarnieri T, Fisherman JS, Christian MC, Donehower R C. Cardiac disturbances during the administration of taxol. J Clin Oncol 1991; 9:1704–1712.
31. Liu XY, Nie YK, Liu Y, Chen M. Cardiovascular protective properties of the natural product eugenol. Eur J Pharmacol 2025; 1003:177929.
32. Peixoto-Neves D, Wang Q, Leal-Cardoso JH, Rossoni LV, Jaggar JH. Eugenol dilates mesenteric arteries and reduces systemic blood pressure by activating endothelial cell TRPV4 channels. Br J Pharmacol 2015; 172:3484–3494.
33. Damiani CEN, Moreira CM, Zhang HT, Creazzo TL, Vassallo DV. Effects of eugenol, an essential oil, on the mechanical and electrical activities of cardiac muscle. J Cardiovasc Pharmacol

2004; 44:688–695.
34. Aktaş İ, Gur FM, Bilgiç S. Protective effect of misoprostol against paclitaxel-induced cardiac damage in rats. Prostaglandins Other Lipid Mediat 2024; 171:106813.
35. El-Sayed EM, Mansour AM, Abd El-Aziz GS. Melatonin mitigates paclitaxel-induced cardiotoxicity in rats through modulation of oxidative stress, inflammation, and apoptosis. Life Sci 2023; 316:121369.
36. Zhang Y, Liu X, Wang H, Li Y. Resveratrol protects against paclitaxel-induced myocardial injury by suppressing oxidative stress and inflammatory signaling in rats. Cardiovasc Toxicol 2022; 22:541–551.
37. Liu C, Wang X, Xu S, Liu M, Cao X. Regulation of autophagy: Insights into O-GlcNAc modification mechanisms. Life Sci 2025; 123547.
38. Zou L, Liao M, Zhen Y, Zhu S, Chen X, Zhang J *et al*. Autophagy and beyond: Unraveling the complexity of UNC-51-like kinase 1 (ULK1) from biological functions to therapeutic implications. Acta Pharm Sin B 2022; 12:3743–3782.